The 2016 World Congress on
The 2016 Structures Congress (Structures16)
Jeju Island, Korea, August 28-September 1, 2016

Seismic Behavior of Prefabricated Composite Columns with Bolt-Connected Steel Angles

*Hyeon-Jin Kim[1)], Hyeon-Jong Hwang[2)] and Hong-Gun Park[3)]

[1),3)] *Department of Architectural Engineering, SNU, Seoul, 08826, Korea*
[2)] *College of Civil Engineering, Hunan University, Hunan, 410082, China*
[1)] *bultanun2@gmail.com*

ABSTRACT

To improve the structural capacity and constructability, a prefabricated steel-reinforced concrete (PSRC) column was developed. In the PSRC column, steel angles are placed at the corners of the cross section and bolt-connected with lateral steel plates. A cyclic loading test was performed on four composite columns to investigate the load-carrying capacity, deformation capacity, and bond strength of the steel angles. The test results showed that the closely spaced steel plates and Z-shaped steel plates increased the bond strength between the steel angles and concrete without bolt connection failure. After cover concrete spalling, the load-carrying capacity of the PSRC columns decreased due to the steel angle buckling.

1. INTRODUCTION

In conventional concrete-encased steel (CES) composite columns, a steel section is placed at the center of the cross-section, which is inefficient to increase the overall flexural capacity of the column [Fig. 1(a)]. For better structural performance of the columns, many researchers have studied the composite section with steel angles at the corners of the cross section. Poon (1999), Montuori and Piluso (2009), and Campione (2013) performed concentric and eccentric compression tests for RC columns strengthened with angles at the corners of the cross section and lateral steel plates (battens or strips). The test results showed that the load-carrying capacity and deformation capacity were improved by using the angles and the lateral steel plates. Eom et al. (2013), and Hwang et al. (2016) developed a prefabricated steel-reinforced concrete column (PSRC) [Fig. 1(b)]. A prefabricated steel cage weld-connected by transverse bars and corner angles was encased in the cover concrete. In the flexural tests performed by Eom et al. (2013), however, the angles subjected to tensile force in

[1)] Graduate Student
[2)] Assistant Professor
[3)] Professor

large inelastic deformation showed early fractures at the weld-connections between the angles and the transverse bars. Furthermore, the weld connection could 1) deteriorate long-term stability of PSRC columns, 2) require expensive labor costs, and 3) limit the use of high-strength steel.

The present study focuses on the bolt-connection between steel angles and lateral steel plates [Fig. 1(c)]. In a newly proposed PSRC column, the bolt-connection method is expected to 1) prevent premature buckling of the steel angles, 2) improve the constructability, and 3) increase bond strength of the steel angle due to bearing between concrete and bolts. The cyclic lateral loading test for three PSRC column specimens and a conventional CES column specimen were performed. Seismic behaviors such as strength, ductility, and energy dissipation capacity were investigated.

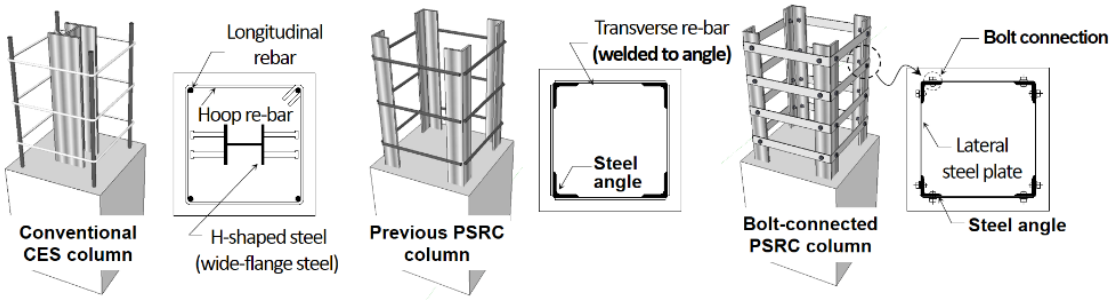

Fig. 1 Concrete-encased composite columns

2. DESIGN OF PSRC COLUMN

2.1 Flexural and Shear Strengths

In accordance with the Korean Building Code: KBC (2009) and American Institute of Steel construction: AISC 360 (2010), the ultimate flexural strength M_n of PSRC columns can be evaluated on the basis of 1) strain compatibility and 2) plastic stress distribution. According to Eom et al. (2013), the shear-resisting contribution of the angles to the shear strength of a PSRC member can be neglected. Thus, according to KBC (2009) and American Concrete Institute: ACI 318 (2011), the nominal shear strength V_n of PSRC columns can be calculated as shown in Eq. (1).

$$V_n = \left[1 + N/\left(14A_g\right)\right]\sqrt{f'_c}\, b/d/6 \quad A_t\, F_{yt} \tag{1}$$

where N = axial force normal to cross section; A_g = gross area of concrete section; b = width of the cross section; d = effective depth of the cross section; and A_{st}, F_{yt}, and s = area, yield stress, and spacing of the lateral steel plates, respectively.

2.2 Bond strength between steel angles and concrete

Fig. 2 shows the bond stress distribution due to bearing of the lateral steel plates and bolt head in a bolt-connection of PSRC column. For conservative design, nominal bond strength B_n of a steel angle can be calculated by ACI 318 (2011) (i.e., frictional

resistance of the angle and contribution of bolt head to concrete bearing were neglected).

$$B_n = n\{0.85 f_c'[\alpha((l_{tb} \times t_{tb}) + (l_b \times t_b))]\} \quad (2)$$

where n = the number of the bolt joints in the angle over the shear span length; l_{tb} = effective length of the lateral steel plates contributing to concrete bearing (i.e., distance between the tip of the angle and the edge of the lateral steel plate, see Fig. 2); t_{tb} = thickness of the lateral steel plates; l_b, t_b = diameter and thickness of the nut tightened with the bolt, respectively; α (≤ 2.0) is a factor addressing the confinement effect on the bearing area.

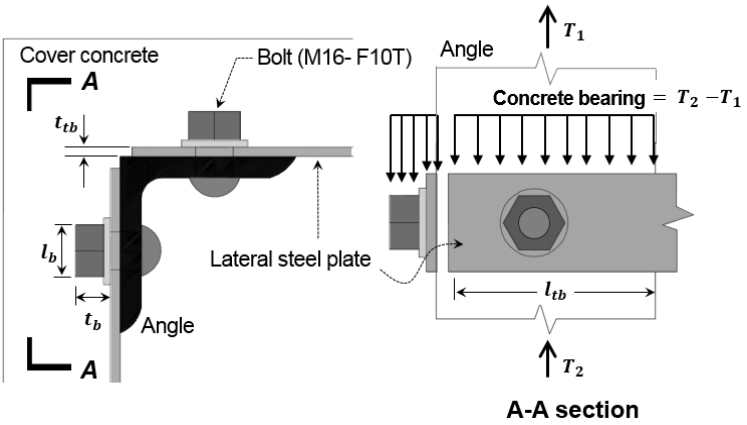

Fig. 2 Bond strength between steel angles and concrete

2.3 Bolt Connection

The lateral steel plates in a bolt-connected PSRC column provide 1) bond strength between the steel angles and concrete and 2) lateral confinement for the core concrete, and 3) shear transfer between the steel angels. Therefore, the fractures of the bolt joints at the both ends of the lateral steel plates should be prevented until the gross section of the lateral steel plate yield. As shown in Fig. 3, according to KBC (2009) and AISC 360 (2010), the failure strength R_n of the bolt connection and the lateral steel plate can be calculated as the minimum strength of Eqs. (3) to (7).

For tensile yielding of gross section, $R_n = F_{yt}A_t$ (3)

For tensile rupture of effective net section, $R_n = F_{ut}A_e$ (4)

For bearing failure at bolt holes, $R_n = 1.5L_c t_r F_{ut} \leq 3.0dt_r F_{ut}$ (5)

For block shear rupture, $R_n = 0.6F_u A_{nv} + F_u A_{nt} \leq 0.6F_u A_{gv} + F_u A_{nt}$ (6)

For shear failure of bolts, $R_n = 0.5F_{ub}A_b$ (7)

where, F_{yt}, F_{ut} = yield stress, tensile stress of the lateral steel plates; A_t, A_e = gross area, effective net area of the lateral steel plates; L_c = clear distance between the edge of the hole and the edge of the connected material; t_r = thickness of the lateral steel plates; d = nominal bolt diameter; A_{gv} = gross area subject to shear (= d_{gv} x t_r); A_{nv} = net area subject to shear (= d_{nv} x t_r); A_{nt} = net area subject to tension (=d_{nt} x t_r); F_{ub} = nominal tensile strength of the bolt; A_b = nominal unthreaded body area of the bolt.

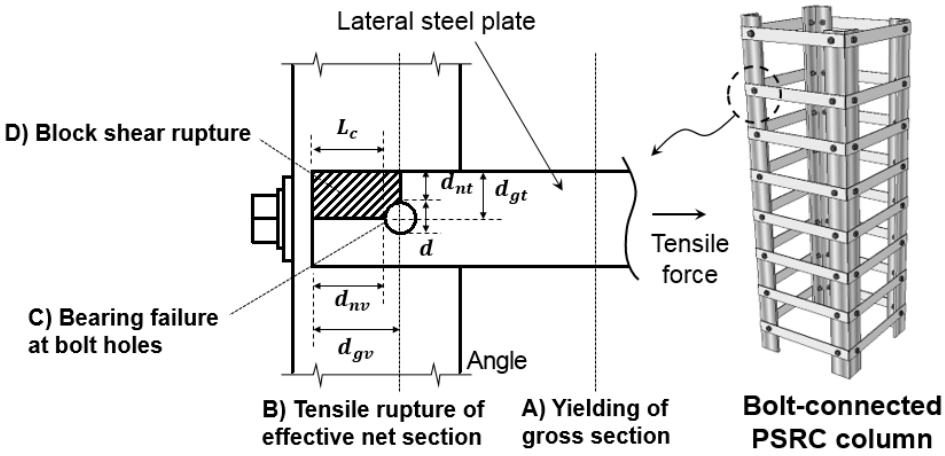

Fig. 3 Failure modes of bolt-connection between the steel angles and lateral steel plates

3. TEST PROGRAM

3.1 Design of test specimens

Table 1 and Fig. 4 show the details and test parameters of a CES specimen S1 and three bolt-connected PSRC column specimens S2-S4. The test parameters were the spacing of lateral steel plates (i.e., 150 mm or 250 mm) and sectional configuration of lateral steel plates (i.e., flat steel plate or Z-shaped steel plate).

Table 1. Specimens for cyclic loading tests

Specimens	Dimensions (mm)	Steel ratio (%)	Longitudinal steel [yield strength (MPa)]	Lateral reinforcements (mm) [yield strength (MPa)]
S1	Cross section: 500 x 500 Column height: 2300	1.9	H-140x140x8x9 (454.0) + 4 D19 (514.7)	D10 @ 150 (446.7)
S2		1.4	4 L-75x75x6 (626.3)	FB-40x3.2 @ 250 (319.7)
S3		1.4		FB-40x3.2 @ 150 (319.7)
S4		1.4		Z-30x50x30 @ 250 (319.7)

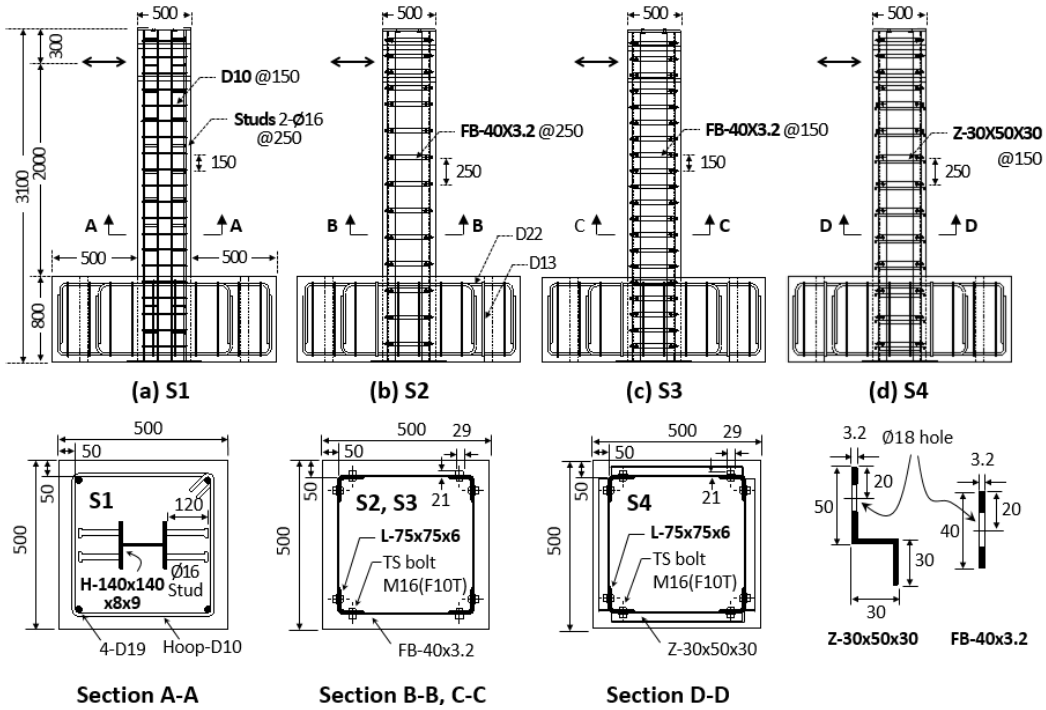

Fig. 4 Dimensions and details of column specimens (unit: mm)

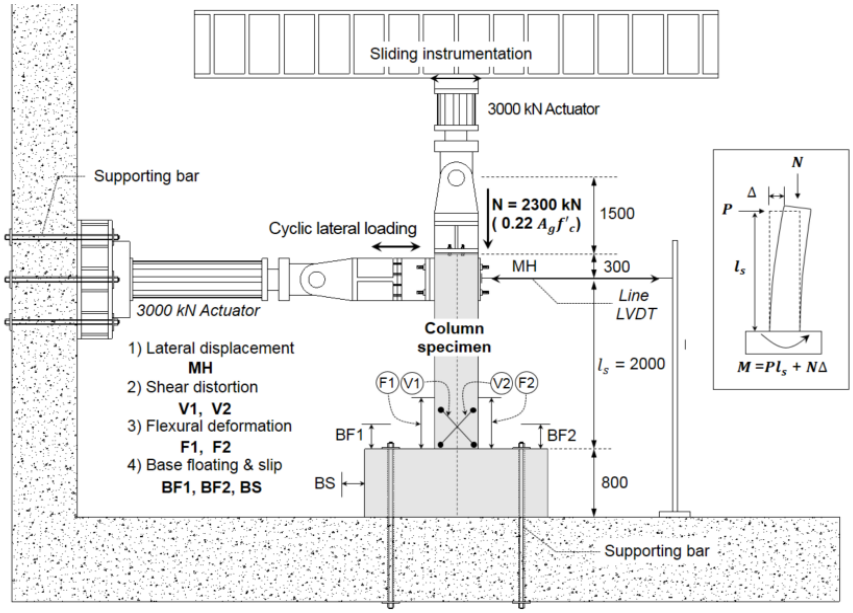

Fig. 5 Test setup

3.2 Material properties and Test method

The yield strength of longitudinal bar, H-shaped steel, steel angle, lateral bars, and steel plate is 514.7, 454.0, 626.3, 446.7, and 319.7 MPa, respectively. The concrete strength at the day of the test was f'_c = 39.9 MPa. As shown in Fig. 5, cyclic

lateral loading was applied to the column specimens under uniform axial compression N = 2300 kN. The cyclic loading protocol was planned according to AISC 360 (2010). Lateral displacement was measured at the loading point.

4. TEST RESULTS

4.1 Lateral load – drift ratio relationship

Fig. 6 shows the lateral load – drift ratio (P-δ) relationships of the specimens. The drift ratio was calculated by dividing the net lateral displacement at the loading point by the effective column height l_s = 2,000 mm. The lateral load-carrying capacities were decreased by the second-order effect of compression force as follows.

$$P_n = P_{no} - N\delta^* \text{ (presented as the dotted line in Fig.6)} \quad (8)$$

where, δ^* is modified drift ratio considering the additional height of the instrumentation between the top surface of the specimens and the hinge of the vertical actuator.

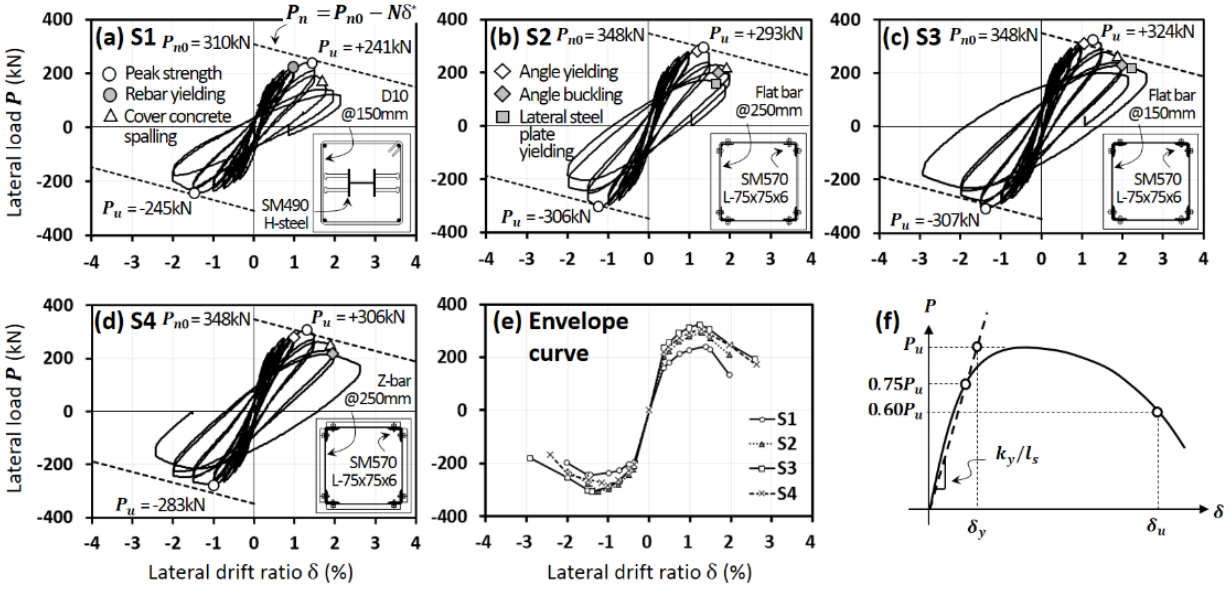

Fig. 6 Lateral load – drift ratio relationships of test specimens

As shown in Fig. 6(f), the yield drift ratio was calculated as $\delta_y = P_u / (k_y l_s)$. where, the yield stiffness k_y = slope corresponding to $0.75P_u$ as indicated by Park (1988), l_s = shear span length of the specimens (= the height of the specimens = 2,000 mm). The ultimate drift ratio δ_u was defined as the post-peak drift ratio corresponding to $0.60P_u$.

The test results showed that the peak strengths of the PSRC specimens were greater than that of the CES specimen. (+241 / −245 kN for S1 and +293 ~ +306 kN /

−283 ~ −307 kN for S2 to S4) This result is because that the corner angles increases the flexural moment capacity. The deformation capacity of PSRC specimen S3 was greater than that of the CES specimen S1, even though the lateral reinforcements of S1 and S3 were equally spaced as 150 mm. In the PSRC specimens, S3 with the lateral flat steel plates at a spacing of 150 mm exhibited greater lateral load-carrying capacity and deformation capacity than those of S1 with the flat steel plates at a spacing of 250 mm. S4 which used the Z-shaped steel plate as a lateral element showed the greater strength and deformation capacity than those of S2 with the lateral flat steel plate, despite the same spacing (=250 mm) of the lateral steel plates. All the PSRC specimens showed greater lateral load-carrying capacity than the predictions by the current design codes (KBC 2009 and AISC 360-10).

4.2 Failure modes

Fig. 7 shows the damage in the plastic hinge regions of the specimens at the lateral drift ratio δ = 2.0%. After the peak strength, the load-carrying capacity of the conventional CES specimen S1 decreased until the lateral load P = 0.60P_u, due to the crushing of the cover concrete and the second-order effect of compression force [Fig. 7(a)]. In the PSRC specimen S2, laterally strengthened with flat steel plates at a spacing of 250 mm, spalling of the cover concrete occurred at the angle surface. Ultimately, S2 failed at δ = 2.0% due to the angle buckling [Fig. 7(b)]. On the other hand, spalling of the cover concrete in S3 and S4 decreased due to the better lateral confinement [Figs. 7(c) and (d)]. In the PSRC specimens, because of the slender section (KBC 2009 and AISC 360-10) of the angle, the steel angle buckling occurred at the end of the tests. The bolt-connections were not failed during the tests.

(a) S1 [δ = 2.0%] (b) S2 [δ = 2.0%] (c) S3 [δ = 2.0%] (d) S4 [δ = 2.0%]

Fig. 7 Failure modes in the plastic hinge zones

5. SUMMARY AND CONCLUSIONS

In the present study, to investigate the seismic behaviors of bolt-connected PSRC columns with various details, cyclic lateral loading tests were performed. From the test results, the load-carrying capacity, deformation capacity, and failure mode were investigated. The main results of the tests are summarized as follows:

(1) Bolt-connected PSRC column specimens showed greater load-carrying capacity than current design code

(2) Due to the steel angles at the corners of the cross section, the load-carrying capacities of the PSRC specimens were 22 - 34% greater than that of the conventional CES specimens.
(3) The bond strength and bolt connection were designed in accordance with the KBC and AISC provisions. Early spalling of the cover concrete and failure of the bolt-connections did not occur in the PSRC column specimens.
(4) In the inelastic deformation range, laterally well-confined columns by the closely spaced lateral steel plates delayed the delamination of the cover concrete. The Z-shaped steel plates provided greater lateral confinement than the flat steel plates due to the better sectional properties, which were efficient to resist tensile force and out-of-plane bending for the confining the core concrete.

REFERENCES

ACI (American Concrete Institute). (2011), "*Building code requirements for structural concrete and commentary*.", *ACI 318-11*, Farmington Hills, MI

AIK (Architectural Institute of Korea). (2009), "*Korean building code*.", Seoul.

AISC. (2010), "Specification for structural steel building.", *ANSI/AISC 360-10*, Chicago.

Campione, G. (2013), "R/C columns strengthened with steel angles and battens; Experimental results and design procedure." *Pract. Period. Struct. Des. Constr.*, Vol. **18**(1), 1-11.

Eom, T.S., Hwang, H.J., Park H.G., Lee, C.N., Kim, H.S. (2013), "Flexural test for steel-concrete composite members using prefabricated steel angles.*" J. Struct. Eng.*, Vol. **140**(4), 04013094.

Hwang, H.J., Eom, T.S., Park, H.G., Lee, C.N. and Kim, H.S. (2016), "Axial load and cyclic lateral load tests for composite columns with steel angles." *J. Struct. Eng.*, Vol. **142**(5), 04016001.

Montuori, R., and Piluso, V. (2009), "Reinforced concrete columns strengthened with angles and battens subjected to eccentric load." *Eng. Struct.*, Vol. **31**(2), 539-550.

Park, R. (1988), "State-of-the-art report on ductility evaluation from laboratory and analytical testing." *Proceedings of 9th World Conference on Earthquake Engineering*, Tokyo.

Poon, E. D. (1999), *Effect of column retrofitting on the seismic response of concrete frames*, Dept. of Civil Engineering and Applied Mechanics, McGill Univ., Montreal.